



Gill filament permeabilization: A novel approach to assess mitochondrial function in sheephead minnows (*Cyprinodon variegatus*) following anthraquinone exposure

DOI:
[10.1016/j.cbpc.2019.108699](https://doi.org/10.1016/j.cbpc.2019.108699)

Document Version
Accepted author manuscript

[Link to publication record in Manchester Research Explorer](#)

Citation for published version (APA):

Reynolds Kirby, A., Galli, G., Crossley, J., Sweet, L. E., Crossley II, D. A., & Roberts, A. P. (2019). Gill filament permeabilization: A novel approach to assess mitochondrial function in sheephead minnows (*Cyprinodon variegatus*) following anthraquinone exposure. *Comparative Biochemistry and Physiology. Part C: Comparative Pharmacology*. Advance online publication. <https://doi.org/10.1016/j.cbpc.2019.108699>

Published in:
Comparative Biochemistry and Physiology. Part C: Comparative Pharmacology

Citing this paper

Please note that where the full-text provided on Manchester Research Explorer is the Author Accepted Manuscript or Proof version this may differ from the final Published version. If citing, it is advised that you check and use the publisher's definitive version.

General rights

Copyright and moral rights for the publications made accessible in the Research Explorer are retained by the authors and/or other copyright owners and it is a condition of accessing publications that users recognise and abide by the legal requirements associated with these rights.

Takedown policy

If you believe that this document breaches copyright please refer to the University of Manchester's Takedown Procedures [<http://man.ac.uk/04Y6Bo>] or contact uml.scholarlycommunications@manchester.ac.uk providing relevant details, so we can investigate your claim.



Comparative Biochemistry and Physiology, Part C

Gill Filament Permeabilization: A Novel Approach to Assess Mitochondrial Function in Sheepshead Minnows (*Cyprinodon variegatus*) following Anthraquinone Exposure --Manuscript Draft--

Manuscript Number:	
Article Type:	Method article
Section/Category:	Crude oil toxicity
Keywords:	Oroboros Oxygraph; Mitochondrial Respiration; ROS Production; Proton Leak; photo-modified PAH; Gill Filaments
Corresponding Author:	Dane Crossley II University of North Texas Denton, TX United States
First Author:	Amanda Reynolds Kirby
Order of Authors:	Amanda Reynolds Kirby Gina L.J. Galli Janna L Crossley Lauren E. Sweet Dane A. Crossley II Aaron P. Roberts
Abstract:	<p>Anthracene is a highly toxic polycyclic aromatic hydrocarbon (PAH), and its toxicity is increased 8-fold after compounding exposure to UV radiation. Exposure to either the parent or photo-modified compound has been shown to cause increases in reactive oxygen species (ROS) production and lipid peroxidation. Since the majority of ROS production occurs within mitochondria, we investigated simultaneous mitochondrial respiration and ROS production in the gills of sheepshead minnows (<i>Cyprinodon variegatus</i>) acutely (48h) exposed to anthraquinone (40 µg l⁻¹). Anthraquinone exposure caused a 25% increase in oxidative phosphorylation with electrons donated to Complex I (OXPHOSCI) and a 33% increase in Leak respiration with oligomycin (Leak-OmyCI). ROS production was slightly increased (33.3%) in Leak state with oligomycin respiring on Complex I substrates (Leak-OmyCI) after anthraquinone exposure, but this value remained unchanged in all other respiratory states. When ROS production was normalized to mitochondrial oxygen consumption, we found that ROS production was decreased in all respiratory states, but most noticeably in the Leak state. We speculate that differences in the antioxidant defense system may have played a role in decreased ROS production. Overall, in this paper we present a novel technique to measure mitochondrial function in the gill filaments of teleost fish exposed to xenobiotic molecules, and we show anthraquinone exposure alters aspects of oxidative phosphorylation and ROS production.</p>
Suggested Reviewers:	Gigi Lau OsloMet - storbyuniversitetet gigi.lau@ibv.uio.no Mitochondrial Researcher Georgina Cox University of Guelph cox@zoology.ubc.ca Environmental Toxicology and Fish Rasphal Dhillon The University of British Columbia dhillon@zoology.ubc.ca Mitochondrial Researcher Andrew Esbaugh University of Texas at Austin

	<p>a.esbaugh@austin.utexas.edu Previous mitochondrial work and environmental toxicology on fish</p>
	<p>Elena Fabbri Universita di Bologna elena.fabbri@unibo.it Researcher in environmental toxicology</p>
	<p>Kevin Brix The University of British Columbia kevinbrix@icloud.com Environmental Toxicology</p>
Opposed Reviewers:	

Dear Dr Grosell,

Please find accompanying this letter our submission of the manuscript entitled: Gill Filament Permeabilization: A Novel Approach to Assess Mitochondrial Function in Sheepshead Minnows (*Cyprinodon variegatus*) following Anthraquinone Exposure for consideration for publication. In this manuscript we discuss our work in developing a novel technique to measure mitochondrial respiration in the gill filaments of a fish exposed to a single PAH. We have made every effort to follow the formatting requirements of CBP C.

Thank you for your consideration.

Dr Dane A Crossley II

- Novel Gill Filament Preparation to Measure Mitochondrial Respiration and ROS Production
- Acute Anthraquinone Exposure Increased Respiration and ROS production in OXPHOS and Leak states
- Observed Results may be Evidence of Mounting Antioxidant Defense Response to Xenobiotic Molecules

1 Gill Filament Permeabilization: A Novel Approach to Assess Mitochondrial Function in
2 Sheepshead Minnows (*Cyprinodon variegatus*) following Anthraquinone Exposure
3

4 A. Reynolds Kirby¹, Gina Galli², Janna Crossley¹, Lauren E. Sweet³ Dane A. Crossley II^{1*},
5 Aaron P. Roberts³
6

7 ¹ Developmental and Integrative Biology Division, Department of Biological Sciences,
8 University of North Texas, Denton, Texas

9 ² Faculty of Medical and Human Sciences, University of Manchester, Manchester, United
10 Kingdom

11 ³ Advanced Environmental Research Institute, Department of Biological Sciences, University of
12 North Texas, Denton, Texas
13

14 *Corresponding Author: Dane A. Crossley II; email: dane.crossley@unt.edu

15 **Abstract**

16 Anthracene is a highly toxic polycyclic aromatic hydrocarbon (PAH), and its toxicity is
17 increased 8-fold after compounding exposure to UV radiation. Exposure to either the parent or
18 photo-modified compound has been shown to cause increases in reactive oxygen species (ROS)
19 production and lipid peroxidation. Since the majority of ROS production occurs within
20 mitochondria, we investigated simultaneous mitochondrial respiration and ROS production in the
21 gills of sheepshead minnows (*Cyprinodon variegatus*) acutely (48h) exposed to anthraquinone
22 ($40 \mu\text{g l}^{-1}$). Anthraquinone exposure caused a 25% increase in oxidative phosphorylation with
23 electrons donated to Complex I (OXPHOS_{CI}) and a 33% increase in Leak respiration with
24 oligomycin (Leak-Omy_{CI}). ROS production was slightly increased (33.3%) in Leak state with
25 oligomycin respiring on Complex I substrates (Leak-Omy_{CI}) after anthraquinone exposure, but
26 this value remained unchanged in all other respiratory states. When ROS production was
27 normalized to mitochondrial oxygen consumption, we found that ROS production was decreased
28 in all respiratory states, but most noticeably in the Leak state. We speculate that differences in
29 the antioxidant defense system may have played a role in decreased ROS production. Overall, in
30 this paper we present a novel technique to measure mitochondrial function in the gill filaments of
31 teleost fish exposed to xenobiotic molecules, and we show anthraquinone exposure alters aspects
32 of oxidative phosphorylation and ROS production.

33

34 **Keywords:** Oroboros Oxygraph; Mitochondrial Respiration; ROS Production; Proton Leak;
35 photo-modified PAH; Gill Filaments

36 **Introduction**

37 Polycyclic aromatic hydrocarbons (PAHs) are a carcinogenic compound found in smoke,
38 tar, and crude oil. PAHs are released into the atmosphere by the burning and distilling of coal ore
39 (Dipple, 1985), and into aquatic environments through the harvesting and transportation of crude
40 oil (Pasparakis et al., 2019). Some PAHs contain photodynamic properties that are responsive to
41 wavelengths in the UVA spectrum (315-400 nm) and can magnify toxicity in aquatic systems,
42 resulting in photo-enhanced toxicity (Roberts et al., 2017). Photodynamic PAHs are excited by
43 UVA light (380 nm), resulting in the formation of excited singlet and triplet state molecules.
44 These molecules are highly reactive with their surrounding media and generate photo-modified
45 PAHs (byproducts), as well as reactive oxygen species (ROS), which enhances overall toxicity
46 leading to oxidative stress (Arfsten et al., 1996; Mallakin et al., 1999). The photo-modified
47 PAHs are typically oxidized, resulting in higher water solubility and bioavailability to aquatic
48 organisms than the parent PAHs. These molecules are highly reactive in tissues and attach to
49 membrane lipids, which compromise cellular and organelle membrane integrity (Sikkema et al.,
50 1994).

51 Without the influence of UV, anthracene is a highly toxic PAH with an LC₅₀ of
52 approximately 16.6 µg l⁻¹, which is enhanced eight-fold (LC₅₀ of 1.94 µg l⁻¹) after co-UV
53 exposure (Weinstein and Polk, 2001). Bluegill sunfish (*Lepomis macrochirus*) exposed to 12 µg
54 l⁻¹ of anthracene resulted in 100% mortality within nine hours of direct UV exposure (Bowling et
55 al., 1983). The photo modification of anthracene (as a result of co-UV exposure) forms over 20
56 toxic byproducts (including anthraquinone), and generally the photoproducts are more toxic than
57 the parent compounds (Mallakin et al., 1999). In the case of anthracene, 50% growth inhibition
58 in aquatic duckweed (*Lemna gibba*) was achieved at a concentration of 1.0 mg l⁻¹, while the

59 same growth inhibition was achieved in lower concentrations (0.1 mg l^{-1}) (Huang et al., 1995).
60 Photodynamic PAHs (anthracene) absorb UV radiation resulting in an excited energy state and
61 oxidized photoproducts (anthraquinone). The energy released as the excited compound returns to
62 the ground state and can be transferred directly to cellular O_2 or membrane lipids (Roberts et al.,
63 2017). This process of photosensitization has been proposed as the mechanism of toxicity (for
64 PAHs and their photoproducts) through the production of reactive oxygen species (ROS),
65 resulting in oxidative damage to tissues and membranes Mallakin et al., 1999; Roberts et al.,
66 2017; Weinstein and Polk, 2001). In fact, markers of oxidative stress (increased lipid
67 peroxidation and ROS production) were found in bluegill sunfish liver microsomes after 60
68 minutes of exposure to anthracene ($3.015 \text{ } \mu\text{g ml}^{-1}$) and UV light (Choi and Oris, 2000).

69 Considering that ROS production occurs in the mitochondrial complexes, we wanted to
70 measure the effects of anthraquinone on mitochondrial function (oxygen consumption and
71 coupling efficiency) while simultaneously measuring ROS production in sheepshead minnow gill
72 filaments. We chose the gill filament as a target tissue because PAHs easily flux across the gill
73 epithelium and are rapidly dispersed into the bloodstream (Ramachandran et al., 2006). In the
74 past, oxidative phosphorylation of the gills has been measured in purified isolated mitochondria.
75 However, this preparation requires large tissue samples, which is not possible in small fish
76 species, such as the sheepshead minnow. To this end, we have developed a novel, whole
77 permeabilized gill filament preparation to assess mitochondrial function and simultaneous ROS
78 production in sheepshead minnows (*Cyprinodon variegatus*) following acute (48h)
79 anthraquinone exposure. Permeabilization of the tissue removes the influence of the antioxidant
80 defense systems and cascade signaling and gives us access to the electron transport chain for
81 pharmacological manipulations (Pesta and Gnaiger, 2012). Here we show that the permeabilized

82 gill preparation is suitable for mitochondrial measurements and can be successfully utilized for
83 toxicological investigations.

84 **Materials and Methods**

85 *Animals*

86 Adult, mix-sexed Sheepshead Minnows (*Cyprinodon variegatus*) were purchased from
87 Aquatic Biosystems (Fort Collins, CO) and overnighted to the University of North Texas. Upon
88 arrival, minnows were housed in 100 l tanks filled with 25 ppt saltwater maintained at 26 °C.
89 Saltwater was mixed in the lab by combining deionized facility water with Instant Ocean® Sea
90 Salt (United Pet Group, Blacksburg, VA). Minnows were kept on a 10:14 hour light:dark
91 photoperiod and fed *Artemia* sp. flake food ad libitum every other day, except 24h prior to
92 experimentation. Water quality (pH [6.8-7.5], ammonia [< 5 ppm], nitrite [< 1.0 ppm], nitrate [$<$
93 40 ppm]) parameters were monitored daily.

94 *Acute (48h) Anthraquinone Exposure*

95 Adult minnows (two per replicate) were moved to 20l exposure tanks filled with 25 ppt
96 saltwater maintained at 26°C. One tank contained anthraquinone ($40 \mu\text{g l}^{-1}$) dissolved in DMSO,
97 and the other tank contained an equal volume of DMSO (dimethyl sulfoxide) to serve as a
98 vehicle control. After 24h, minnows were transferred to new aquaria that were filled with 25 ppt
99 saltwater and a dose of either anthraquinone ($40 \mu\text{g l}^{-1}$) or DMSO (equal volume). A 48h static
100 renewal exposure is a fairly standard procedure when assessing compound toxicity and is used as
101 a precaution of biodegradation and volatilization (Weinstein and Polk, 2001). The concentration
102 of anthraquinone used in this study is within environmentally relevant levels (less than $10 \mu\text{g ml}^{-1}$
103 ¹) for anthracene and related byproducts. Temperature and oxygen saturation were monitored
104 throughout experimentation using a handheld YSI dissolved oxygen probe (YSI, Inc, Yellow

105 Springs, OH). Water parameters (pH, ammonia, nitrate, and nitrate) were monitored throughout
106 the exposure period. After 48h, the trial was terminated and minnows were euthanized using a
107 lethal dose of buffered MS-222 (100mg l⁻¹ MS-222 and 200 mg l⁻¹ NaHCO₃). Gill baskets were
108 removed from both sides of the fish and immediately processed according to the procedures
109 below.

110 *Permeabilized Gill Filament Preparation*

111 Gill arches were placed in ice-cold BIOPS (pH 7.1) containing [2.8 mM CaK₂EGTA (pH
112 7.0), 7.2 mM K₂EGTA (pH 7.0), 5.8 mM Na₂ATP, 6.6 mM MgCl₂·6H₂O, 20 mM Taurine, 15
113 mM Na₂ Phosphocreatine, 20 mM Imidazole, 0.5 mM Dithiothreitol, and 50 mM 2-(N-
114 morpholino) ethanesulfonic acid] (Galli et al., 2016). Under a Lecia EZ4 dissecting scope (Lecia
115 Microsystems Inc., Buffalo Grove, IL) with a dark background, mucous and blood clots were
116 removed from the gill arches (figure 1). Gill arches were incubated at 4°C in BIOPS with
117 saponin (50 µg ml⁻¹) on an orbital shaker (Cole-Parmer, Vernon Hills, IL) for 12 minutes at
118 speed two. Arches were triple washed (to remove excess lipids) for 10 minutes in 4°C MIR05
119 respiration medium (pH 7.1) containing [0.5 mM EGTA, 3.0 mM MgCl₂·6H₂O, 60 mM K-2-(N-
120 morpholino) ethanesulfonic acid, 20 mM Taurine, 10mM KH₂PO₄, 20mM HEPES, 110 mM D-
121 Sucrose, 1% BSA] (Galli et al., 2016). Gill filaments were cut from the arches and wet weight
122 was recorded. Gill filaments (wet weight 2 mg) were added to each chamber of an Oroboros
123 Oxygraph 2K HR respirometer (Oroboros Instruments, Innsbruck, Austria) containing MIR05
124 respiration solution maintained at 30°C. The chambers were hyper-oxygenated and oxygen
125 concentration was maintained between 200-400 nm ml⁻¹ during each trial. Mitochondrial
126 function analyses were conducted in two parts: 1) measurement of mitochondrial respiration with
127 simultaneous ROS production and 2) a cytochrome c test with measurement of OXPHOS_{CIV}.

128 This was done because cytochrome c and TMPD with ascorbate (complex IV substrates) are
129 strong redox substances that consume H₂O₂ which interferes with the H₂O₂ calibration and
130 overall sensitivity of the method (Makrecka-Kuka et al., 2015).

131 The Oroboros was outfitted with O2K-fluorescence LED probes (Oroboros Instruments,
132 Innsbruck, Austria) to detect ROS flux within the Oxygraph chambers. The following protocol
133 measuring simultaneous ROS production and mitochondrial respiration is modified from
134 previously published studies (Krumshnabel et al., 2015; Suski et al., 2012). AmplexTM UltraRed
135 (10 μM), horseradish peroxidase (1 U/ml), and superoxide dismutase (10 U/ml) were injected
136 into each chamber to induce oxidation of AmplexTM UltraRed to red-fluorescent resorufin in the
137 presence of H₂O₂. The fluorescent signal was calibrated by stepwise injections of 400 μM H₂O₂
138 (final concentration; 0-2 mM).

139 *Protocol 1: Respiratory states and ROS production*

140 Respiratory substrates malate (2 mM) and pyruvate (5 mM) were injected into the
141 chambers and served as a measurement for LEAK respiration without adenylates while respiring
142 on Complex I substrates (LEAK-LN_{CI}; table 1). Succinate (10 mM) was added to the chamber to
143 measure LEAK respiration with Complex I and II substrates without adenylates (LEAK-
144 LN_{CI+CI}; table 1). OXPHOS_{CI+CI} (table 1) was induced by adding saturating levels of ADP (5
145 mM). Oligomycin (2 μg ml⁻¹) was then added to the chambers to block the ATP synthase and
146 measure LEAK state with Oligomycin (LEAK-Omy_{CI+CI}; table 1). Rotenone (0.5 μM) was
147 titrated into the chambers to inhibit Complex I of the ETS and measure LEAK-Omy_{CI} (table 1).
148 Lastly, Antimycin A (2.5 μM) was added to the chambers to measure residual oxygen
149 consumption (ROX) or chamber respiration not attributed to mitochondrial respiration (table 1).

150

151 *Protocol II: Cytochrome C test and OXPHOS_{CIV} Respiration*

152 Malate (2mM), and pyruvate (5mM) were added to provide carriers for the citric acid
153 cycle. Saturating concentrations of ADP (5mM) were injected into the chambers to initiate
154 OXPHOS_{CI}, and succinate (10 mM) was added to provide substrates for complex II activation
155 (OXPHOS_{CI+CII}; table 1). Cytochrome c (10 μM) was added to assess mitochondrial quality and
156 to determine inner mitochondrial membrane integrity after permeabilized gill filament
157 preparation (table 1). OXPHOS_{CIV} was stimulated through tetramethyl-p-phenylene-diamine
158 (TMPD; 0.5mM) and ascorbate (2 mM) injections (table 1).

159 *Calculations and Statistical Analysis*

160 Trials were excluded from the data analysis when respiration rate increased above 15%
161 after cytochrome c injection and when respiratory control ratios (RCR) were lower than 6, which
162 indicated a damaged preparation (Brand, 2011). All fluxes were corrected for background O₂
163 consumption by subtracting the respiration rate after gills were added but before mitochondrial
164 substrates and inhibitors were added. Respiration rate and ROS production were normalized to
165 the wet weight of the gill filaments and expressed as pmol sec⁻¹ mg wet wt⁻¹. The respiratory
166 control ratio (RCR) was calculated by dividing OXPHOS_{CI+CII} respiration rate by LEAK_{LNCI+CII}
167 in protocol I. All statistical tests were performed using Statistica Version 13.3. A repeated-
168 measures ANOVA with a Tukey HSD test was used to make comparisons in mitochondrial
169 respiration and ROS production between treatments. A student's t-test was used to check for
170 difference at OXPHOS_{CIV} and RCRs between control and exposed minnows.

171 **Results and Discussion**

172 To date, the effects of individual PAH exposure on intact mitochondrial function are
173 relatively unknown. Few studies have highlighted the effects of crude oil exposure on

174 mitochondrial function, which provided the framework for our investigation. We have developed
175 a new preparation for measuring mitochondrial function in whole gill preparations from small
176 fish. Furthermore, we have shown exposure to anthraquinone effects aspects of mitochondrial
177 electron transport chain function and ROS production.

178 *Development of a permeabilized whole-gill mitochondrial preparation*

179 Permeabilized mitochondrial preparations allow detailed characterization of electron
180 transport chain function in their normal intracellular position, thus preserving essential
181 interactions with the cytoskeleton and other organelles. We adapted protocols for skeletal muscle
182 preparations to develop a permeabilized whole-gill preparation (Fig. 1A). Our RCR values
183 (control: 3.88 ± 0.49 and exposed: 4.42 ± 0.42) from permeabilized gill filaments are consistent
184 with published values in teleost cardiac and skeletal muscle (Fig. 1B; Chung et al., 2017;
185 Guderley and Johnston, 1996; Iftikar and Hickey, 2013). Furthermore, there were negligible
186 effects of Cytochrome C, which suggests the inner mitochondrial membrane was intact. Taken
187 together, these results suggest the fibers were of excellent quality with no overt signs of
188 dysfunction from the permeabilization process (Brand, 2011). Therefore, we consider this
189 preparation is appropriate for studying mitochondrial function in whole-gills, which is
190 particularly useful for studies in small fish.

191 *Effects of anthraquinone on Electron Transport Chain Function and ROS production*

192 There was a tendency for anthraquinone exposure to cause an increase in oxygen
193 consumption across all respiratory states. This effect was particularly pronounced, and
194 statistically significant, when Complex I and II substrates were combined in both the OXPHOS
195 and Leak-Omy states (Fig. 1B). The fact that both Leak and OXPHOS increased with
196 anthraquinone exposure meant that RCR's ratios were similar between exposed minnows and

197 controls (3.88 ± 0.49 and 4.42 ± 0.44 respectively), suggesting that mitochondrial efficiency
198 remained unchanged. These results suggest anthraquinone exposure increases mitochondrial
199 oxidative capacity in minnows. Given that ATP demand is increased during toxic exposure (e.g.,
200 recruitment of ATP-dependent ion channels), a greater mitochondrial capacity may represent a
201 compensatory mechanism to match ATP supply to demand during environmental stress.

202 Anthraquinone exposure led to a 30% increase in ROS production during Leak-Omy_{CI+CII}
203 respiratory state (Fig. 1D). However, a different pattern emerged when ROS production was
204 normalized to mitochondrial oxygen consumption. For all leak respiratory states (Leak-Ln_{CI},
205 Leak-Omy_{CI+CII}, Leak-Omy_{CII}), ROS production was reduced by 20 to 40% in mitochondria from
206 minnows exposed to anthraquinone (Fig 1E). Therefore, after differences in oxygen consumption
207 are taken into account, our results suggest ROS production is lower in minnows exposed to
208 anthraquinone, compared to controls. While we did not address the mechanism underlying the
209 differences in ROS production, it is possible that minnows exposed to anthraquinone may mount
210 a protective response by actively suppressing pathways involved in ROS production, or
211 upregulating the antioxidant defense system (Regoli et al., 2011). Support for the latter
212 hypothesis comes from studies in liver mitochondria of goldfish (*Carassius auratus*), which
213 showed levels of superoxide dismutase and catalase were elevated in exposed to phenanthrene
214 exposure (a PAH that is abundant in aquatic systems) (Yin et al., 2007). Nevertheless, it is
215 possible that the exposure length or concentration was not long or high enough to overwhelm
216 the antioxidant defense system, leading to an increase in ROS production, similar to previous
217 studies (Yin et al., 2007). Further research is necessary to resolve these speculations, which
218 could include measurements of antioxidants and markers of oxidative damage (lipid
219 peroxidation).

220 In contrast to our study, Xu and colleagues (2017) found that larval red drum (*Sciaenops*
221 *ocellatus*) exposed to crude oil concentrations of $4.8 \mu\text{g l}^{-1}$ ΣPAH_{50} at 24h, 48h, and 72h had
222 differential transcription profiles that were consistent with changes in mitochondrial function,
223 mitochondrial transmembrane potential, oxidative stress response pathways, and cell death
224 signaling (Xu et al., 2017). In adult red drum, mitochondrial function and performance was
225 assessed following 24h exposure at concentrations of $29.6 \pm 7.4 \mu\text{g l}^{-1}$ and $64.5 \pm 8.9 \mu\text{g l}^{-1}$
226 ΣPAH_{50} and they found no change in Leak respiration, maximal ETS, or coupling controls ratios
227 (markers of mitochondrial dysfunction) after 24h of crude oil exposure (Johansen and Esbaugh,
228 2019). Mitochondrial function has also been measured in adult Mahi-mahi (*Coryphaena*
229 *hippurus*) that were exposed to crude oil ($9.6 \pm 1.7 \mu\text{g l}^{-1}$ ΣPAH_{50}) for 24h and the authors
230 determined that while $\text{OXPHOS}_{\text{CI}}$ and $\text{OXPHOS}_{\text{CII}}$ respiration was decreased, classic markers of
231 mitochondrial dysfunction were not observed (no change in leak respiration, maximal ETS, or
232 coupling control ratios) (Kirby et al., 2019). It should be mentioned that the crude oil
233 concentrations used in the 24h exposures are environmentally relevant to concentrations that
234 occurred during the Deepwater Horizon Oil Spill (Wade et al., 2011) and the lowest doses were
235 previously shown to affect swim performance and aerobic scope in adult fish (Johansen and
236 Esbaugh, 2017; Mager et al., 2014). Taken together, these studies and ours suggest the effects of
237 crude oil and their constituents on fish mitochondrial function are variable and unpredictable.
238 Clearly, more research needs to be conducted in other areas of mitochondrial bioenergetics to
239 determine the mechanisms of toxicity that crude oil and individual PAH have on teleost
240 mitochondrial function.

241

242

243 **Acknowledgments**

244 This research was made possible by a grant from The Gulf of Mexico Research Initiative. Data

245 are publicly available through the Gulf of Mexico Research Initiative Information & Data

246 Cooperative (GRIIDC) at <https://data.gulfresearchinitiative.org> (doi: 10.7266/N71Z4304).

247

248 **Tables and Figure Legends**

249 **Table 1:** The action and subsequent mitochondrial states as a result of substrates and inhibitors
 250 used in Protocol I and II.

	Action	State	Electron Entry	Abbreviation
PROTOCOL I				
Malate (2 mM) pyruvate (5 mM)	Citric acid cycle and glycolysis intermediates. Substrates for Complex I-linked respiration	LEAK respiration without adenylates (LN)	Complex I	LEAK-LN _{CI}
Succinate (10mM)	Citric acid cycle intermediate. Substrate for Complex II-linked respiration	LEAK respiration without adenylates (LN)	Complex I & II (convergent electron entries into the Q-junction)	LEAK-LN _{CI+CII}
Saturating ADP (5mM)	Substrate for ATP synthase	OXPHOS respiration	Complex I & II	OXPHOS _{CI}
Oligomycin (2 µg ml ⁻¹)	Inhibitor of the F ₁ F ₀ ATPase (Complex V)	LEAK state induced with oligomycin	Complex I & II	LEAK-Omy _{CI+CII}
Rotenone (0.5 µM)	Inhibitor of Complex I	LEAK state induced with oligomycin	Complex II	LEAK-Omy _{CII}
Antimycin A (2.5 µM)	Inhibitor of Complex III	Residual oxygen consumption	N/A	ROX
Respiratory Control Ratio	Indicates the degree of coupling OXHPOS and ATP synthase	OXPHOS _{CI-CIV} / Leak-LN _{CI+CII}	N/A	RCR
PROTOCOL II				
Malate (2 mM) pyruvate (5 mM)	Citric acid cycle and glycolysis intermediates, respectively. Substrates for Complex I-linked respiration	LEAK respiration without adenylates (LN)	Complex I	LEAK-LN _{CI}
ADP (5mM)	Substrate for ATP synthase	OXPHOS respiration	Complex I & II	OXPHOS _{CI}
Succinate (10mM)	Citric acid cycle intermediate. Substrate for Complex II-linked respiration	LEAK respiration without adenylates (LN)	Complex I & II	OXPHOS _{CI+CII}
Cytochrome C (10 µM)	Component of the electron transport chain	N/A	N/A	N/A
Ascorbate (2mM)	Antioxidant to prevent autoxidation of TMPD (see next step)	N/A	N/A	N/A
Tetramethyl-p-phenylene-diamine (TMPD; 0.5mM)	Electron donor to Complex IV	OXPHOS respiration	Complex IV	OXPHOS _{CIV}

252 Figure 1: Gill arches (A) extracted from a Sheepshead Minnow (*Cyprinodon variegatus*) and
253 viewed under a Lecia EZ4 dissecting scope prior to permeabilization. Protocol one
254 measurements of mitochondrial respiration (B) and simultaneous ROS production (D) after 48h
255 of exposure in control tanks (open bars) or in anthraquinone (40 µg l⁻¹) dosed tanks (closed bars).
256 Measurements from protocol two on OXPHOS respiration (C). ROS production normalized for
257 mitochondrial respiration rate (E). Data are represented as means ± s.e. Single asterisk denotes
258 significant differences between treatments (p < 0.05).

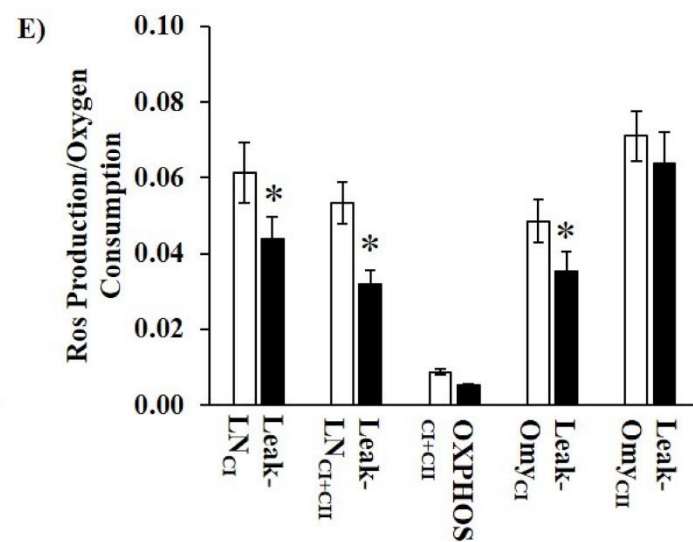
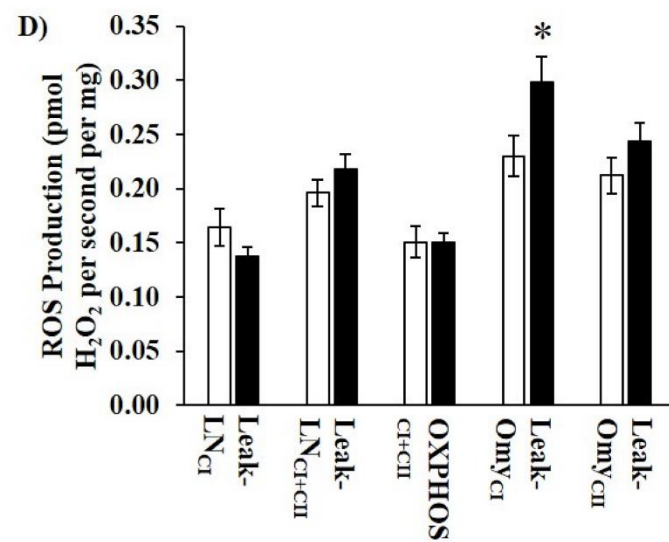
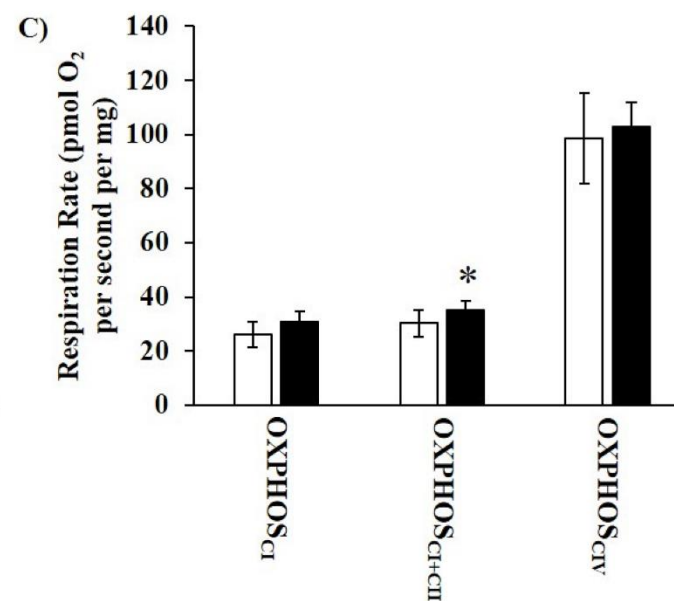
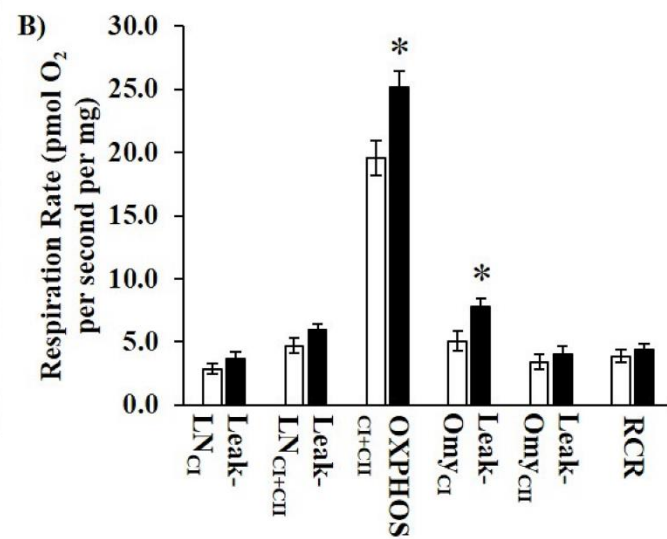
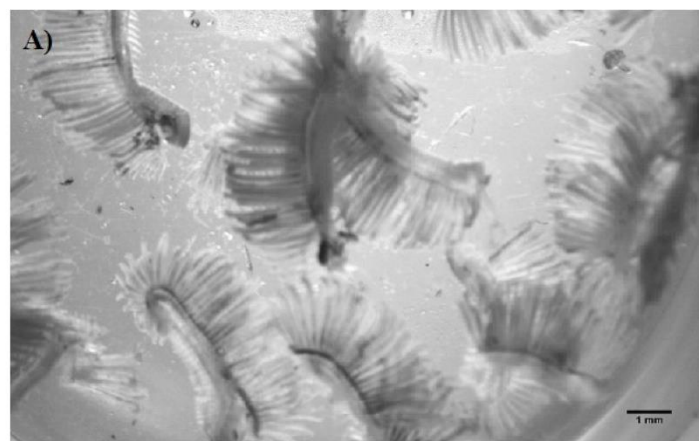
259 References

- 260 1. Arfsten, D. P., Schaeffer, D. J., & Mulveny, D. C. (1996). The Effects of Near Ultraviolet
261 Radiation on the Toxic Effects of Polycyclic Aromatic Hydrocarbons in Animals and
262 Plants: A Review. *Ecotoxicology and Environmental Safety*, 33(1), 1-24.
263 doi:http://dx.doi.org/10.1006/eesa.1996.0001
- 264 2. Brand, M.D. and Nicholls, D. G., 2011. Assessing mitochondrial dysfunction in cells.
265 *Biochemical Journal*, 435(Pt 2), 297-312. doi:10.1042/BJ20110162
- 266 3. Bowling, J., Leversee, G., Landrum, P., & Giesy, J. (1983). Acute mortality of
267 anthracene-contaminated fish exposed to sunlight. *Aquatic Toxicology*, 3(1), 79-90.
- 268 4. Choi, J., and Oris, J. T., 2000. Evidence of oxidative stress in bluegill sunfish (*Lepomis*
269 *macrochirus*) liver microsomes simultaneously exposed to solar ultraviolet radiation and
270 anthracene. *Environmental Toxicology and Chemistry*, 19(7), 1795-1799.
271 doi:10.1002/etc.5620190713
- 272 5. Chung, D.J., Bryant, H.J., Schulte, P.M., 2017. Thermal acclimation and subspecies-
273 specific effects on heart and brain mitochondrial performance in a eurythermal teleost
274 (*Fundulus heteroclitus*). *The Journal of Experimental Biology* 220, 1459-
275 1471.
- 276 6. Dipple, A. (1985). Polycyclic Aromatic Hydrocarbon Carcinogenesis. 283, 1-17.
277 doi:10.1021/bk-1985-0283.ch001
- 278 7. Galli, G.L.J., Crossley, J., Elsey, R.M., Dzialowski, E.M., Shiels, H.A., Crossley, D.A.,
279 2016. Developmental plasticity of mitochondrial function in American alligators,
280 *Alligator mississippiensis*. *American Journal of Physiology - Regulatory,*
281 *Integrative and Comparative Physiology* 311, R1164-R1172.
- 282 8. Guderley, H., Johnston, I., 1996. Plasticity of fish muscle mitochondria with thermal
283 acclimation. *Journal of Experimental Biology* 199, 1311-1317.
- 284 9. Huang, X.D., Dixon, D.G., Greenberg, B.M., 1995. Increased Polycyclic Aromatic
285 Hydrocarbon Toxicity Following Their Photomodification in Natural Sunlight: Impacts
286 on the Duckweed *Lemna gibba* L. G-3. *Ecotoxicology and Environmental Safety* 32,
287 194-200.

- 288 10. Iftikar, F.I., Hickey, A.J.R., 2013. Do Mitochondria Limit Hot Fish Hearts?
289 Understanding the Role of Mitochondrial Function with Heat Stress in *Notolabrus*
290 *celidotus*. PLOS ONE 8, e64120.
- 291 11. Johansen, J.L., Esbaugh, A.J., 2017. Sustained impairment of respiratory function and
292 swim performance following acute oil exposure in a coastal marine fish. *Aquatic*
293 *Toxicology* 187, 82-89.
- 294 12. Johansen, J.L., Esbaugh, A.J., 2019. Oil-induced responses of cardiac and red muscle
295 mitochondria in red drum (*Sciaenops ocellatus*). *Comparative Biochemistry and*
296 *Physiology Part C: Toxicology & Pharmacology* 219, 35-41.
- 297 13. Kirby, A.R., Cox, G.K., Nelson, D., Heuer, R.M., Stieglitz, J.D., Benetti, D.D., Grosell,
298 M., Crossley, D.A., 2019. Acute crude oil exposure alters mitochondrial function and
299 ADP affinity in cardiac muscle fibers of young adult Mahi-mahi (*Coryphaena hippurus*).
300 *Comparative Biochemistry and Physiology Part C: Toxicology & Pharmacology* 218, 88-
301 95.
- 302 14. Krumschnabel, G., Fontana-Ayoub, M., Sumbalova, Z., Heidler, J., Gauper, K., Fasching,
303 M., & Gnaiger, E. (2015). Simultaneous high-resolution measurement of mitochondrial
304 respiration and hydrogen peroxide production. *Methods Mol Biol*, 1264, 245-261.
305 doi:10.1007/978-1-4939-2257-4_22
- 306 15. Mager, E.M., Esbaugh, A.J., Stieglitz, J.D., Hoenig, R., Bodinier, C., Incardona, J.P.,
307 Scholz, N.L., Benetti, D.D., Grosell, M., 2014. Acute embryonic or juvenile exposure to
308 Deepwater Horizon crude oil impairs the swimming performance of mahi-mahi
309 (*Coryphaena hippurus*). *Environ Sci Technol* 48, 7053-7061.
- 310 16. Mallakin, A., McConkey, B.J., Miao, G., McKibben, B., Snieckus, V., Dixon, D.G.,
311 Greenberg, B.M., 1999. Impacts of structural photomodification on the toxicity of
312 environmental contaminants: anthracene photooxidation products. *Ecotoxicology and*
313 *Environmental Safety* 43, 204-212.
- 314 17. Makrecka-Kuka, M., Krumschnabel, G., and Gnaiger, E., 2015. High-Resolution
315 Respirometry for Simultaneous Measurement of Oxygen and Hydrogen Peroxide Fluxes
316 in Permeabilized Cells, Tissue Homogenate and Isolated Mitochondria. *Biomolecules*,
317 5(3), 1319-1338. doi:10.3390/biom5031319
- 318 18. Pasparakis, C., Esbaugh, A. J., Burggren, W., & Grosell, M., 2019. Impacts of deepwater
319 horizon oil on fish. *Comparative Biochemistry and Physiology Part C: Toxicology &*
320 *Pharmacology*, 224, 108558. doi:https://doi.org/10.1016/j.cbpc.2019.06.002
- 321 19. Pesta, D. and Gnaiger, E., 2012. High-Resolution Respirometry: OXPHOS Protocols for
322 Human Cells and Permeabilized Fibers from Small Biopsies of Human Muscle # *T*
323 *Mitochondrial Bioenergetics* (Vol. 810, pp. 25-58).
- 324 20. Ramachandran, S.D., Swezey, M.J., Hodson, P.V., Boudreau, M., Courtenay, S.C., Lee,
325 K., King, T., Dixon, J.A., 2006. Influence of salinity and fish species on PAH uptake
326 from dispersed crude oil. *Marine pollution bulletin* 52, 1182-1189.
- 327 21. Regoli, F., Giuliani, M.E., Benedetti, M., Arukwe, A., 2011. Molecular and biochemical
328 biomarkers in environmental monitoring: A comparison of biotransformation and
329 antioxidant defense systems in multiple tissues. *Aquatic Toxicology* 105, 56-66.
- 330 22. Roberts, A.P., Alloy, M.M., Oris, J.T., 2017. Review of the photo-induced toxicity of
331 environmental contaminants. *Comparative Biochemistry and Physiology Part C:*
332 *Toxicology & Pharmacology* 191, 160-167.

- 333 23. Sikkema, J., de Bont, J. A., & Poolman, B., 1994. Interactions of cyclic hydrocarbons
334 with biological membranes. *Journal of Biological Chemistry*, 269(11), 8022-8028.
- 335 24. Suski, J. M., Lebiezinska, M., Bonora, M., Pinton, P., Duszynski, J., and Wieckowski,
336 M. R., 2012. Relation between mitochondrial membrane potential and ROS formation.
337 *Methods Mol Biol*, 810, 183-205. doi:10.1007/978-1-61779-382-0_12
- 338 25. Wade, T.L., Sweet, S.T., Sericano, J.L., Guinasso, N.L., Diercks, A.R.R., Highsmith,
339 R.C., Asper, V.L., Joung, D.D., Shiller, A.M., Lohrenz, S.E., 2011. Analyses of water
340 samples from the Deepwater Horizon oil spill: Documentation of the subsurface plume.
341 *Monitoring and Modeling the deepwater horizon oil spill: a record-breaking enterprise*,
342 77-82.
- 343 26. Weinstein, J.E., Polk, K.D., 2001. Phototoxicity of anthracene and pyrene to glochidia of
344 the freshwater mussel *Utterbackia imbecillis*. *Environmental Toxicology and Chemistry*
345 20, 2021-2028.
- 346 27. Xu, E.G., Khursigara, A.J., Magnuson, J., Hazard, E.S., Hardiman, G., Esbaugh, A.J.,
347 Roberts, A.P., Schlenk, D., 2017. Larval Red Drum (*Sciaenops ocellatus*) Sublethal
348 Exposure to Weathered Deepwater Horizon Crude Oil: Developmental and
349 Transcriptomic Consequences. *Environmental Science & Technology* 51, 10162-10172.
- 350 28. Yin, Y., Jia, H., Sun, Y., Yu, H., Wang, X., Wu, J., Xue, Y., 2007. Bioaccumulation and
351 ROS generation in liver of *Carassius auratus*, exposed to phenanthrene. *Comparative*
352 *Biochemistry and Physiology Part C: Toxicology & Pharmacology* 145, 288-293.

Figure



□ Control
 ■ Anthraquinone Exposed

Disclosures

No conflicts of interest, financial or otherwise, are declared by the author(s).